JBUON 2021; 26(5): 1815-1823
ISSN: 1107-0625, online ISSN: 2241-6293 • www.jbuon.com
Email: editorial_office@jbuon.com

ORIGINAL ARTICLE

Joint prediction of solitary pulmonary nodule malignant probability based on logistic regression and malignant tendency comprehensive score

Shutong Zhou[1]*, Qun Wang[2]*, Tianyu Tang[1], Meizhu Cao[1], Yan Tan[1], Kaixian Bai[1], Wenjun Liu[1]

[1]School of Mathematics and Statistics, Nanjing University of Information Science & Technology, China. [2]Department of Pulmonary Medicine, Zhongda Hospital, School of Medicine, Southeast University, China.

*These authors contributed equally to this work and both should be considered co-first authors.

Summary

Purpose: *We analyzed the relationship between clinical data, tumor markers, chest high-resolution CT (HRCT) and pathology in patients with solitary pulmonary nodules (SPN) and explored the joint discrimination scheme to improve the accuracy of noninvasive diagnosis.*

Methods: *242 SPNs with the largest diameter <2cm were divided into training set (161 cases) and test set (81 cases). We screened the risk factors by single factor analysis. Then, we established the prediction equation model (PE model) based on logistic regression and malignant tendency comprehensive score model (MTCS model) based on the evaluation criteria of SPN. The weight of the two sub models was used to determine the joint evaluation model (JE model).*

Results: *Age, CEA content, maximum diameter, pleural adhesions, spicule sign, and ground glass component were independent factors of malignant prediction ($p<0.05$) recorded as x_1~x_6, and PE model was established as $P_1=e^x/(1+e^x)$,$x=0.052x_1+0.0327x_2+0.212x_3+1.849x_4+1.066x_5+1.769x_6-7.582$. According to the different performance of different manifestations of the corresponding score, we could get each score of SPN. The MTCS model was S/8.5. The JE model was $P=0.76P_1+0.24S/8.5$. The results of the test set showed the AUC values of JE, PE, MTCS, Mayo, VA and Li Yun model for D ≤2cm SPN were 0.930 (95% CI:0.877-0.983), 0.922 (95% CI:0.870-0.974), 0.900 (95% CI:0.879-0.921), 0.782 (95% CI:0.749-0.815), 0.744 (95% CI:0.731-0.756) and 0.801 (95% CI:0.739-0.863). The sensitivity of JE, PE, MTCS model was 87.2%, 79.2%, 73.3%, the specificity was 90.1%, 89.2%, 82.2%, and the accuracy was 89.9%, 85.5%, 81.2%.*

Conclusions: *The joint evaluation model has better diagnostic efficiency and can provide reference for the diagnosis of SPN with D≤2cm.*

Key words: *joint evaluation model, malignant tendency comprehensive score model, prediction equation model, solitary pulmonary nodule*

Introduction

Solitary pulmonary nodule (SPN) usually refers to a circular or circular-like lesion surrounded by the lung parenchyma with a diameter ≤3cm that exists independently in the lung, without atelectasis, enlarged hila, or pleural effusion, etc. performances [1]. Studies have shown that for primary early lung cancer (stage IA) with a diameter ≤3cm and no metastasis, the 5-year survival rate of patients after surgery reaches 70-80% [2]. As an important evidence for the diagnosis of early lung cancer, the differentiation of benign and malignant SPN is vital. Only the earlier diagnosis and treat-

Corresponding author: Wenjun Liu, PhD. School of Mathematics and Statistics, Nanjing University of Information Science & Technology. 219 Ningliu Rd, 210044 Nanjing, China.
Tel: +86 2558695612; Fax:+86 2558731160; Email: wjliu@nuist.edu.cn; wjliu.cn@139.com
Received: 30/03/2021; Accepted: 22/04/2021

ment can better improve the prognosis of patients. In recent years, many researchers have made great progress in using mathematical models to predict the benign and malignant behavior of SPN. Li et al [3] established a prediction model using Logistic regression. This model confirmed that age, maximum diameter, genetic history, calcification, spicule sign, and boundary were risk factors for distinguishing SPN malignancy, which had good clinical application value. On this basis, many researchers have obtained different prediction models by including different sign information. For example, Zhang et al [4] incorporated tumor markers into the prediction model and the accuracy of model prediction improved to some extent. At the same time, with advanced CT equipment, more and more small nodules are discovered A. Dalli et al [5] investigated the diagnostic value of PET/CT in differentiating benign from malignant SPNs. The multivariate linear equation established by Bao [6] could independently predict SPNs with diameter ≤2cm. The pleural indentation sign, vascular bundle sign and spicule sign of SPN were independent risk factors of this model. This model has more advantages in image signs. The VA model and the Mayo model [7] which is popular around the world are less applicable to cases in some regions.

Current studies show that the identification of benign and malignant SPNs is mostly based on a single method, and each method has its own advantages and disadvantages [7]. In the meantime, with the advancement of CT technology and people's increasing concern about their own physical conditions, the detected SPN is mostly ≤2cm in diameter. Some studies have shown that SPN patients with a diameter ≤2cm have no obvious clinical symptoms, but have a higher malignancy detection rate [2, 7-9]. SPN malignant prediction depends on precise image data analysis to reflect the physiology, anatomy and other information of the lesions. In this study, a joint SPN discriminant model with diameter≤2cm was established based on the data of 242 SPN patients confirmed by surgical pathology in Zhongda Hospital, Southeast University, China and then the cohort was evaluated for the diagnostic value of the model.

Methods

The study was approved by the Zhongda Hospital Southeast University Clinical Research Ethics Committee. All the patients signed the informed consent form.

General information

According to the inclusion and exclusion criteria, patients with SPN who visited Zhongda Hospital, Southeast University from May 2018 to May 2019 were retrospectively analyzed. Inclusion criteria: (1) patients with SPN confirmed by surgical pathology in this hospital; (2) SPN maximum diameter ≤2cm; (3) patients with complete clinical data and laboratory examination data; (4) routine lung HRCT scans before surgery. Exclusion criteria: (1) mediastinal lymphadenopathy of the corresponding pulmonary segment and lobes or multiple pulmonary nodules accompanied by pneumonia, atelectasis; (2) treatment history of pulmonary nodules before surgery; (3) incomplete or low-quality CT images.

242 SPNs with the largest diameter <2cm were divided into Group A (161 cases) and Group B (81 cases). Group A was used as the training set to establish the model and determine the model parameters, while Group B was used as the test set to verify the universality and practicability of the model. A total of 161 cases (group A) were finalized, with 86 males and 75 females, aged 25-82 years. There were 107 malignant nodules, including 93 adenocarcinomas, 8 squamous cell carcinomas, and 6 others. There were 54 benign nodules, 33 hamartomas, 12 tuberculomas, and 9 others. In addition, 81 cases (group B) of SPN confirmed by pathology from May 2019 to December 2019 were collected. There were 54 malignant nodules, including 40 adenocarcinomas, 10 squamous cell carcinomas, and 4 others. There were 27 benign nodules, 17 hamartomas, 6 tuberculomas, and 4 others.

CT image acquisition

A 64-slice spiral CT scanner (Philips Brilliance 64-slice CT scanner) was used to routinely scan the patient's lung tip to the costophrenic angle. Breathing phase: end-inspiratory breath scanning. Scanning parameters: working voltage 120kV, working current 100mA, layer thickness 1.25mm, spacing 5mm, scanning matrix 512×512. After the scan, the lung algorithm (window width 1500HU, window level -650HU) image reconstruction was performed using the lung algorithm, and the mediastinal window (window width 350HU, window level 50HU) image reconstruction was performed using the Stand algorithm, with a reconstruction layer thickness of 1 mm.

CT imaging signs

The evaluation of the CT image signs of the cases was carried out randomly when the pathological results were unknown, and was completed by experienced radiologists. The detailed radiographic signs of pulmonary nodules mainly included: (1) Nodule size: the longest and shortest diameter of the nodule; (2) Nodule site: the nodule located in the upper or lower lobe or the right middle lobe of the left and right lung [10]; (3) Nodules types: according to the proportion of ground-glass opacity (GGO), the nodules were divided into solid nodules and sub solid nodules, the latter including mixed ground-glass nodules and pure ground-glass nodules [10]; (4) Vacuole sign: air-like low-density shadow of diameter ≤5cm inner the nodule lesion [11]; (5) Lobular sign: the contour of the nodule presented multiple arcs with unevenness, mainly including no obvious lobulation (nodular edges smooth or nearly smooth), shallow lobulation and obvious lobulation [6]; (6) Spicule sign:

radial line shadow at the junction of lung nodules and lung parenchyma [11]; (7) Pleural adhesions sign: linear or wide basal depression between the edge of the lung nodule and the adjacent pleura [11]; (8) Vascular bundle sign: the vascular structure in the lungs gathered toward the nodule, mostly manifested as blood vessels cross the nodule or shift towards the nodule [10].

Clinical and laboratory examination data

The clinical data, such as gender, age, smoking history and family genetic history, were collected. The contents of 4 tumor markers (CEA, NSE, CYFRA 21-1 and ProGRP patients) [12] were detected.

By analogy to the definition method of smoking index, we defined the open flame cooking index as the daily cooking frequency×the number of cooking years. Then we defined the occupational risk level, and the occupational risk level for dust-exposed occupations, such as chemical factory workers, teachers, traffic police and cooks, as level 1. Others were level 2.

We then defined the external environmental risk index that leads to SPN malignancy. When the smoking index was >400 or the open flame cooking index was >40 or the occupational risk level was level 1, the external environment risk level was level 1. When the smoking index was less than 400 or the open flame cooking index was less than 40 or the occupational risk level was level 2, the external environment risk level was level 2.

Statistics

SPSS25.0, MATLAB 2016 and R software were used for statistical analysis of the data. (1) Binary or multiclass assignment of variables of different classes;(2) Single factor was used to analyze the relationship between each factor and the benign and malignant SPN. Risk factors for benign and malignant SPN lesions were determined by T-test or rank sum test. On this basis, the nomogram of SPN malignant tendency was obtained. Based on the experience of doctors and other literature, the scoring criteria for malignant tendency of SPN signs were established. (3) Establish SPN malignant prediction equations according to risk factors. The probability of malignancy of SPN in each patient was calculated and compared with the pathological diagnosis. The optimal threshold was determined according to the Youden index. Reactive oxygen species (ROC) curve was established to compare the difference between the actual result and the predicted result. (4) The SPN malignant tendency score criteria were used to determine the score of each nodule, and the optimal threshold were obtained by comparing with the pathological diagnosis results. (5) The optimal weight and threshold were determined to obtain the final joint discrimination model. The joint model was compared with the submodel and the existing model, and the ROC curve was drawn. The results of the training set and the test set were compared using Delong test. At the same time, the Decision Curve Analysis (DCA) curve was drawn to compare the two submodels of the joint discriminant model.

Results

Screening of risk factors

We analyzed the degree of influence of various factors on the benign and malignant pulmonary nodules, and found that patients' age, CEA content, SPN maximum diameter, pleural adhesions, spicule sign, and ground glass component had statistical significance ($p<0.05$). Gender, smoking

Table 1. Significance test of SPN clinical features, imaging features and serum tumor markers

Index	*Benign* *n (%)*	*Malignant* *n (%)*	t/F/x^2	*p*
Age, years	47.5±3.8	63.5±3.5	-4.906	<0.001
CEA	2.8567	5.2567	2.669	0.039
Maximum diameter	22.677	24.677	5.102	<0.001
Bronchial inflation sign			12.136	<0.001
Yes	5 (16.7)	101 (76.9)		
No	25 (83.3)	30 (23.1)		
Pleural adhesions			5.584	0.018
Yes	5 (16.7)	91 (69.2)		
No	25 (83.3)	41 (30.8)		
Spicule sign			3.868	0.049
Yes	0 (0)	55 (42.3)		
No	30 (100)	76 (57.3)		
GGO			9.260	0.010
Solid nodule	10 (33.3)	17 (12.8)		
Mixed ground- glass	10 (33.3)	39 (29.5)		
Pure ground- glass	10 (33.4)	75 (57.7)		

history, NSE, location of pulmonary nodules, vascular bundle sign, vacuole sign had no statistical significance for SPN benign or malignant (Table 1).

Establishment of prediction equation model

Constructed prediction equation of benign and malignant pulmonary nodules:

$$P_1=e^x/(1+e^x) \quad (1)$$

$$x(D\leq 2cm)=0.052x_1+0.327x_2+0.212x_3+1.849x_4+1.066x_5+1.769x_6-7.582 \quad (2)$$

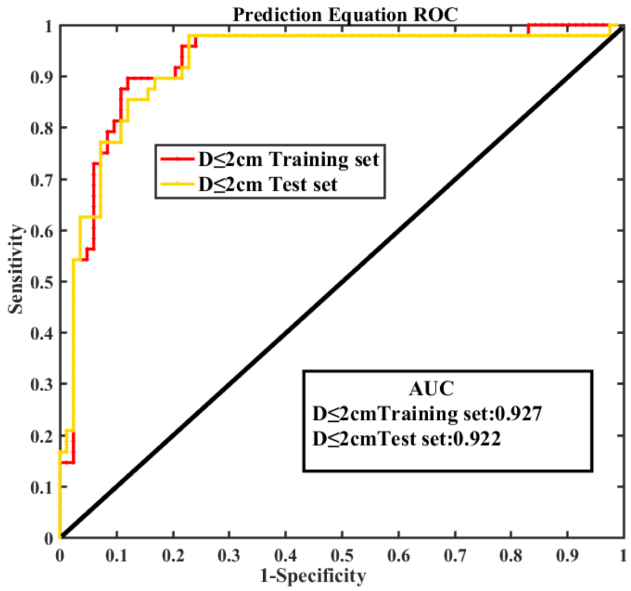

Figure 1. Comparison of ROC curve between SPN training set and test set (prediction equation).

x_1~x_6 are the patients' age, CEA content, SPN maximum diameter, pleural adhesions, spicule sign, and ground glass component.

For the SPN ≤2cm, the AUC with 95%CI of the ROC curve of the model were 0.927, 0.879~0.976, and the optimal cut-off point was 0.4671032. At this time, the sensitivity, specificity and accuracy of the model were 83.3%, 89.2% and 87% respectively (Figure 1). The test set was substituted into the model for verification, and the prediction model ROC curve AUC was 0.922 (95%CI: 0.870~0.975), and the optimal cutoff point was 0.508211. At this time, the sensitivity, specificity and accuracy of the model were 79.2%, 89.2% and 85.5% respectively (Figure 1).

Based on the model, a visual nomogram can be obtained (Figure 2).

Establishment of SPN malignant tendency comprehensive score system

According to the degree of contribution to malignancy of each sign of SPN (Figure 2), the malignant tendency scoring criteria of SPN were established by combining the prior experience of doctors and the existing research results [9] (Table 2).

For the SPN ≤2cm, the AUC with 95%CI of the ROC curve of the model were 0.907, 0.857~0.956, and the optimal scoring threshold was 3.5. The sensitivity, specificity and accuracy of the model were respectively 76.47%, 88.75% and 83.9% (Figure 3). The test set was substituted into the model for validation. The ROC curve had an AUC of 0.900

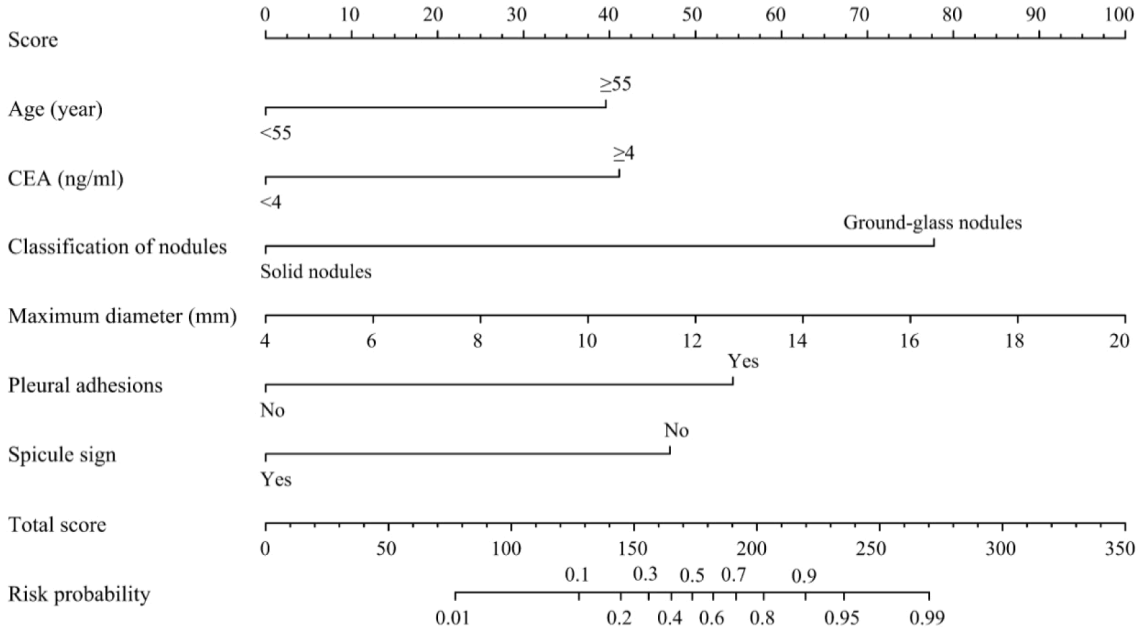

Figure 2. Prediction equation model nomogram.

(95%CI: 0.879~0.921), and an optimal scoring threshold of 3.5. At this time, the sensitivity, specificity and accuracy of the model were 73.3%, 82.2% and 81.2% respectively (Figure 3).

Establishment of joint discriminant evaluation system

Different weights were assigned to the prediction equation model and the malignant tendency comprehensive score model respectively, and the prediction accuracy and the optimal prediction threshold under different weights were calculated (Figure 4).

Based on this, a joint discriminant model could be obtained:

$$P=0.76P_1+0.24S/8.5 \quad (3)$$

When the weights of the prediction equation model and the malignant tendency comprehensive score model were 0.76 and 0.24 respectively, the model got the highest accuracy rate, reaching

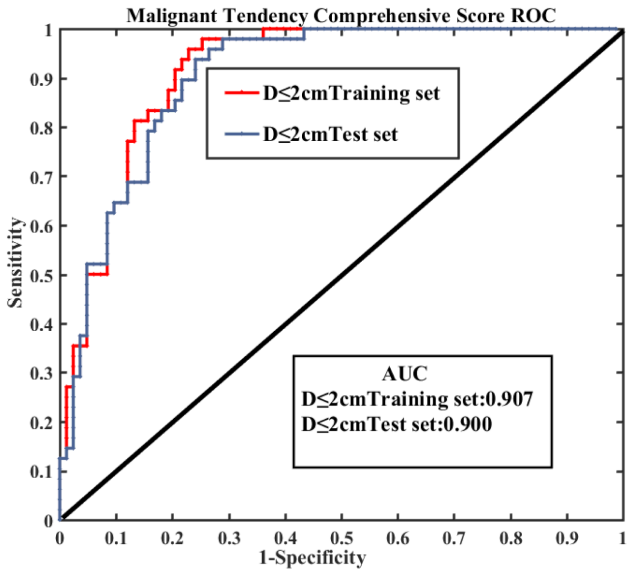

Figure 3. Comparison of ROC curve between SPN≤2cm training set and test set (malignant tendency comprehensive score model).

Table 2. SPN signs malignant tendency score criteria

Score	*Index age*	*Score*	Index
			CEA
0	≤35	0	CEA≤2.5
0.5	35<d<50	0.5	2.5<CEA≤5.5
1	>50	1	CEA>5.5
	maximum diameter		GGO ingredients
0	d≤1cm	0	solid nodule
0.5	1cm<d≤2cm	1	mixed ground -glass
1	d>2cm	2	PGGO
pleural stretch sign		Blur sign	
0	no	0	No
2	yes	1.5	Yes

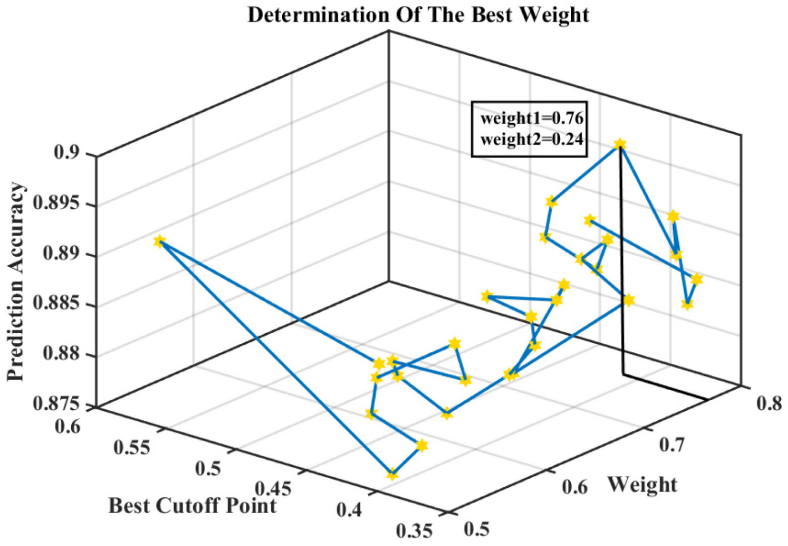

Figure 4. Weight determination of prediction equation model and malignant tendency comprehensive score model.

89.9%, and the threshold was 0.4009306618. If the probability of malignancy was greater than the threshold, it was a malignant nodule; otherwise it was benign (Figure 5).

We compared the results of the joint evaluation model with the prediction equation model, malignant tendency comprehensive score model, Mayo model, VA model, and Li Yun model and substituted the test set data into each prediction model to obtain the results (Table 3), and draw their ROC curves (Figure 6).

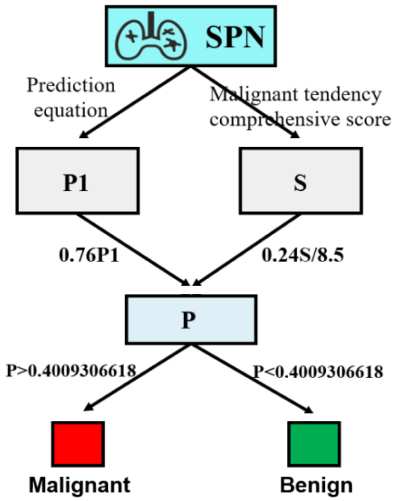

Figure 5. SPN benign and malignant joint discrimination evaluation system.

The AUC of the joint evaluation model, prediction equation model, malignant tendency comprehensive score model, Mayo model, VA model, and Li Yun model were 0.930, 0.922, 0.900, 0.782, 0.744 and 0.801, respectively. According to the Z test, the AUC value of this model was statistically significantly different from that of other models ($p<0.05$).

The analysis showed that the joint evaluation model had a good overlap between the calibration curve and the ideal curve in the training set and the verification set, with a high degree of calibration ($p>0.05$) (Figure 7).

Comparing the effects of the malignant tendency comprehensive score model and the prediction equation model (Figure 8), we could see that within a large Pt range, the benefits of the prediction equation model and malignant tendency comprehensive score model were much higher than the extreme curve and the optional Pt range was larger. In the

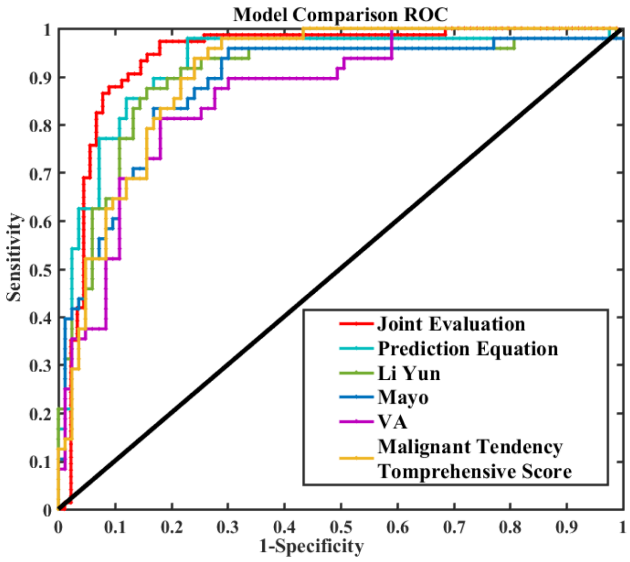

Figure 6. Comparison of prediction model ROC curve.

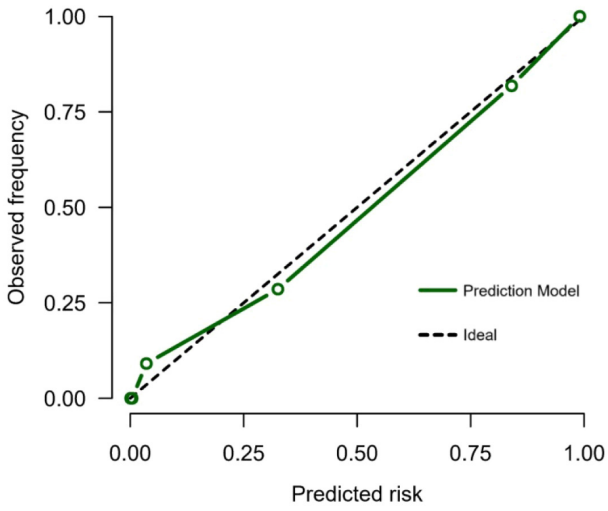

Figure 7. D≤2cm calibration curve of joint evaluation model test set.

Table 3. Comparison of various models of SPN≤2cm

	AUC	*95%CI*	Sensitivity	Specificity	Accuracy	p
Joint evaluation model	0.930	0.877~0.983	87.2%	90.1%	89.9%	0.76
Prediction equation model	0.922	0.870~0.974	79.2%	89.2%	85.5%	0.72
Malignant tendency comprehensive score model	0.900	0.879~0.921	73.3%	82.2%	81.2%	0.71
Mayo model	0.782	0.749~0.815	72.5%	74.2%	73.6%	0.59
VA model	0.744	0.731~0.756	71.2%	74.5%	72.3%	0.53
Li Yun model	0.801	0.739~0.863	75.2%	73.1%	74.5%	0.67

meantime, the prediction equation model was better than the malignant tendency comprehensive score model.

Discussion

With the progress of CT scanning technology, the detection rate of SPNs is increasing year by year, while the spicule sign, vacuole sign, vascular bundle sign and other signs of SPN can be well displayed. SPN is an important basis for the diagnosis of early lung cancer, and its non-invasive diagnosis is of great significance for improving the overall survival rate and reducing the economic cost of lung cancer patients.

At present, there are many mathematical models for SPN prediction, including Li Yun model, Mayo model, VA model, etc. These models mainly study SPN with diameter ≤3cm, and some models narrow the research scope. For example, Bao et al [6] established a multiple linear prediction model for SPN with diameter ≤2cm. Yan et al [13] studied SPN with diameter ranging from 5-15mm. And, most of the models are composed of a single prediction equation. The joint method can overcome some shortcomings of the single method and improve the accuracy. Based on these two points, a joint evaluation model of SPN with diameter ≤2cm is proposed.

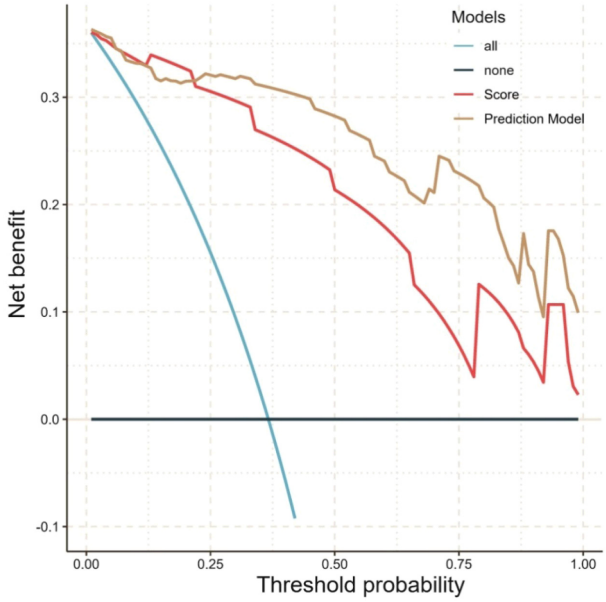

Figure 8. DCA of prediction equation and malignant tendency comprehensive score model.

We analyzed the clinical data, tumor markers, and chest high-resolution CT of SPN patients with the maximum diameter ≤2cm, respectively, and studied the degree of malignant tendency of each sign, and obtained the difference of each sign in the benign and malignant groups (Table 1). On this basis, the malignant tendency score criteria were determined, and the malignant tendency comprehensive score model and prediction equation model were obtained. We can directly see the difference of the contribution rate of different manifestations signs to the malignant degree of pulmonary nodules (Table 4, Figure 2), and establish a joint discriminant model to provide some reference for the diagnosis of SPN.

The ground-glass shadow in SPN is focal ground-glass nodular (fGGN) [14]. According to the proportion of GGO components, the nodules can be divided into solid and sub solid, the latter including mixed ground-glass and pure ground-glass. Some authors think that local ground-glass shadow was a necessary condition for the diagnosis of malignant nodules [15], and further judge according to the edge and internal structure of nodules. The results of Henschke et al [16] showed that the malignant probability of sub solid nodules was higher than that of solid nodules. In this study, it could be seen from the nomogram that the nodule density was closely related to the benign and malignant of SPN. The higher the GGO component, the higher the SPN malignant probability and the OR value of mixed ground -glass and PGGO component was 6.318, indicating that the appearance of local ground-glass shadow increased the SPN

Table 4. Results of binary logistic regression analysis

Index	*β*	*OR*	*95% CI*		*p*
			upper	*lower*	
Age	0.052	1.074	1.032	1.115	0.049
CEA	0.327	1.386	1.048	1.834	0.022
Maximum diameter	0.212	1.236	1.058	1.444	0.008
Pleural adhesions	1.849	6.352	2.031	19.87	0.001
Spicule sign	1.067	2.905	1.675	12.51	0.041
GGO	1.769	6.318	3.217	9.682	0.001

malignant probability, which was consistent with the above conclusions.

Swensen [17] and Muram et al [18] thought that the distribution of SPN in the upper lobe of the lung was more likely to be malignant. In this study, the location of pulmonary nodules was divided by lower lobe and non upper lobe, left lung and right lung in univariate analysis. The results of both groups showed that there was no significant relationship between the location of pulmonary nodules and benign and malignant, which was inconsistent with the results of references. The reason for this result may be that pulmonary tuberculosis is more common in China than in western countries, and is more common in the upper lobe of the lung, leading to an increase in the number of benign pulmonary nodules, so the location of benign and malignant pulmonary nodules is not obvious [19].

Varoli [20] and Vazquez et al [21] believed that the possibility of malignant lesions of nodules will increase with the age of patients, and many models include age into risk factors [1,19]. The results of this study showed that the malignant probability of nodules increased with the age of patients, which was consistent with the references.

The results of Bekci et al [22,23] showed that the sensitivity and specificity of CEA to SPN were 55% and 80%, respectively. The results of this study showed that the OR value of CEA is 1.386, which could be used as a risk factor to distinguish benign and malignant SPN.

The factor of smoking history was not included in the model in this study, which was inconsistent with VA model, Mayo model and Li Yun model, which were widely used at present. This may be due to the large proportion of non-smokers in the data set, with only 28.38% of patients in the smoking malignant group.

The analysis results of ROC curve showed that the accuracy of the joint evaluation model was the highest, and the accuracy of the prediction equation model was slightly higher than that of the malignant tendency comprehensive score model.

In the actual clinical diagnosis, the smaller the nodule, the more difficult to diagnose the benign and malignant subtypes. The results of Wahidi et al [2] showed that the possibility of malignant lesions of pulmonary nodule with diameter >2cm was 64-82%, and the SPN sign with diameter≤2cm was less obvious than that with diameter >2cm, while the number of SPN with diameter≤2cm was more. Therefore, in this paper, a benign and malignant differentiation model was established for SPN with diameter≤2cm. We combined the two prediction models and gave different weights to the two submodels, which, to a certain extent, make up for the shortcomings of the single model and improve the prediction accuracy. However, there are two shortcomings in this model. First, the data volume of this model was limited, and the data were from a single hospital, which could not take into account the regional differences.

Second, the risk factors that could be taken into account in this model were limited. The patient's histological information, such as acini and other factors [24,25] related to the benign and malignant SPN were not included in the model, which may have a certain impact on the accuracy of the model. Improvements are needed in the future. Finally, the CT images in this paper were obtained from 64-slice Spiral CT scanner. The influence of imaging effect of different scanners on the accuracy of discriminating benign and malignant is worth exploring [26].

Acknowledgements

STZ and QW conceived the idea of the study. STZ, QW, TYT and MZC contributed to the design of the research. All authors contributed to data acquisition and interpretation. STZ, TYT and MZC drafted the manuscript. STZ and WJL revisited the manuscript. All authors edited and approved the final version of the manuscript.

This work was supported by the National Natural Science Foundation of China (11771216), the Key Research and Development Program of Jiangsu Province (Social Development) (BE2019725) and the National Undergraduate Innovation & Entrepreneurship Training Program (201910300038).

Conflict of interests

The authors declare no conflict of interests.

References

1. Zhang XH, Chen C, Zeng H et al. Establishment of a clinical predictive model for estimating the malignant probability of solitary pulmonary nodules. J Pract Cancer 2016:31:59-62 (In Chinese).

2. Wahidi MM, Covert JA, Goudar RK et al. Evidence for the treatment of patients with pulmonary nodules: When is lung cancer?: ACCP evidence-based clinical practice guidelines (2nd edition). Chest 2007;132:94s-107s.
3. Li Y, Chen KJ, Sui XC et al. Establishment of a mathematical prediction model for the benign and malignant judgment of solitary pulmonary nodules. J Peking Univers(Health Sciences), 2011;43:450-4 (In Chinese).
4. Zhang M. Establishment of benign and malignant predictive model of solitary pulmonary nodules. South Med Univers, 2016 (In Chinese).
5. Dalli A, Selimoglu S H, Coskunsel M et al. Diagnostic value of PET/CT in differentiating benign from malignant solitary pulmonary nodules. JBUON 2013;18:935-41.
6. Bao Y, Chen FM. Preliminary quantitative study on the discrimination of benign and malignant solitary pulmonary nodules. J Clin Radiol 2019;38:1847-51 (In Chinese).
7. Bao T, Xiao F, Guo YQ et al. Verification, comparison and improvement of the probabilistic prediction model for solitary pulmonary nodules. Chin J Clin Thor Cardiovasc Surg 2018;25:471-6 (In Chinese).
8. Lin NE, Wu S, Wang K et al. Computed tomography quantitative analysis of components: a new method monitoring the growth of pulmonary nodule. Acta Radiol 2013;54:904-8.
9. Macmahon H, Austin JH, Gamsu G et al. Guidelines for management of small pulmonary nodules detected on CT scans: a statement from the Fleischner Society. Radiology 2005;237:395-400.
10. Zhang WD, Shi HC. Evaluation of risk factors for benign and malignant solitary pulmonary nodules. Chin J Clin Thoracic and Cardiovasc Surg 2014;21:532-6 (In Chinese).
11. Yang YH. ROC analysis and clinical application value of benign and malignant comprehensive imaging diagnosis of solitary pulmonary nodules. Shandong University, 2011 (In Chinese).
12. Wang L, Wu CY, Lou JT. The value of tumor marker detection in the differential diagnosis of solitary nodules in the lungs. Mod Immunol J 2016;36:405-9 (In Chinese).
13. Yan RY, Li HX, Ding YY et al. Establishment and verification of benign and malignant predictive models of solitary pulmonary nodules. Radiol Pract 2020;35:352-9 (In Chinese).
14. Lim HJ, Ahn S, Lee KS et al. Persistent pure ground-glass opacity lung nodules≥10mm in diameter at CT scan histopathologic comparisons and prognostic implications. Chest 2013;144:1291-9.
15. Li Q, Liu SY, Fan L et al. MDCT manifestations of malignant focal ground glass density lesions of lungs under 3 cm. J Pract Radiol 2011;27:689-93 (In Chinese).
16. Henschke CI, Yankelevitz DF, Mirtcheva R et al. CT screening for lung cancer: frequency and significance of part-solid and nonsolid nodules.AJR 2002;178:1053.
17. Swensen SJ, Yamashita K, Mccollough CH et al. Lung nodules: Dual-kilovolt peak analysis with CT-Multicenter study. Radiology 2000;214:81-5.
18. Winer-Muram HT, Jennings SG, Tarver RD et al. Volumetric growth rate of stage I lung cancer prior to treatment: serial CT scanning. Radiology 2002;223:798-805.
19. Bai C, Choi CM, Chu CM et al. Evaluation of pulmonary nodules: clinical practice consensus guidelines for Asia. Chest 2016;150:887-93.
20. Varoli F, Vergani C, Caminiti R et al. Management of solitary pulmonary nodule. Eur J Cardiothorac Surg 2008;33:162-5.
21. Vazquez M, Carter D, Brambilla EA et al. Solitary and multiple resected adenocarcinomas after CT screening for lung cancer: Histopathologic features and their prognostic implications. Lung Cancer 2009;64:148-54.
22. Shi TS, Lin RB, Chen C et al. The value of serum CEA, Ca199, Ca125 and Cyfra21-1 in the diagnosis of solitary pulmonary nodules. J Pract Med 2011;27:432-4.
23. Bekci TT, Senol T, Maden E. The efficacy of serum carcinoembryonic antigen (CEA), cancer antigen125 (CA125), carbohydrate antigen 19-9 (CA19-9), carbohydrate antigen 15-3 (CA15-3), alpha fetoprotein (AFP) and human chorionic gonadotropin (HCG) levels in determining the malignancy of solitary pulmonary nodules. J Int Med Res 2009;37: 438- 45.
24. Wachuła E, Szabłowska-Siwik S, Czyżewski D et al. Emphysema affects the number and characteristics of solitary pulmonary nodules identified by chest low-dose computed tomography. A study on screenees with high-risk lung cancer recruited in Upper Silesia. Pol Arch Intern Med 2020;130:17-24.
25. Wu, Z., Huang, T., Zhang, S et al. A prediction model to evaluate the pretest risk of malignancy in solitary pulmonary nodules: evidence from a large Chinese southwestern population. J Cancer Res Clin Oncol 2021;147:275-85.
26. Xia G, An C, Ming Z et al. 18F-FDG-PET/CT versus 99Tcm-MIBI-SPECT: which is better for detection of solitary pulmonary nodules? JBUON 2017;22:1246-51.